Structural and mechanical properties of radiofrequency N/H cold plasma-nitrided C38 carbon steel

F.Z. Bouanis, F. Bentiss, M. Traisnel, C. Jama

Structural and Mechanical properties of Radiofrequency N_2/H_2 cold plasma nitrided C38 carbon steel

F.Z. Bouanis [1,a], F. Bentiss [2], M. Traisnel [1] and C. Jama [1]

[1]Université Lille Nord de France, F-59000 Lille - ENSCL, Unité Matériaux Et Transformations (UMET), UMR 8207, 59650 Villeneuve d'Ascq Cedex, France
[2]Laboratoire de Chimie de Coordination et d'Analytique, Faculté des Sciences, Université Chouaib Doukkali, B.P. 20, M-24000 El Jadida, Morocco

[a] *e-mail: Fatima.bouanis@polytechnique.edu*

Abstract.

C38 carbon steel has been nitrided by radiofrequency cold plasma discharge with the aim to study the effect of gas composition on structural and mechanical properties of nitrided substrates. The plasma nitriding was carried out on unheated substrates, using two different gas mixtures (75% N_2/25% H_2 and 25% N_2/75% H_2) for 8 hours of plasma treatment. Electron Probe Microanalysis (EPMA) showed that the nitrogen content and the nitride layer thickness mainly depend on the hydrogen content in the plasma. For 75%N_2/25%H_2 mixtures, nitrided samples showed the formation of thicker nitride layer with high content of nitrogen compared to those formed in the case of 25% N_2/75% H_2 or pure N_2. The thickness of the nitride layer formed is approximately 15 µm for 8 h of plasma with 75% N_2/25% H_2. X-ray photoelectron spectroscopy (XPS) was employed to obtain chemical-state information of the plasma nitrided steel surfaces. The mechanical properties of plasma nitrided C38 steel were investigated by Vickers microhardness measurements. The micromechanical results show the formation of a new hard layer on the surface after N_2/H_2 treatment plasma and it reaches a maximum value of more than 2242 $HV_{0.005}$ for 75% N_2/25% H_2 plasma nitrided samples. However, a decrease in the hardness values with the applied load has been evidenced.

Keywords: Radiofrequency Cold plasma nitriding ; Hydrogen; C38 carbon steel; Electron Probe Microanalysis; XPS; Microhardness.

1 Introduction

Nitriding is a thermochemical process that is typically used to diffuse nitrogen into ferrous materials. Depending on the plasma nitriding parameters and the material composition, the nitriding process produces a compound layer and a diffusion layer. The compound layer contains iron nitrides such as γ-Fe_4N and/or ε-$Fe_{2-3}N$. The diffusion zone, located between the compound one and the bulk of the metal, consists of nitrogen enriched ferrite. These produced layers can significantly improve surface hardness, fatigue strength, wear and corrosion resistance [1–4]. Plasma nitriding has found wide application in industry [1,2] due to a number of advantages such as a lower process temperature, a shorter treatment time, minimal distortions and a low energy compared to conventional techniques.

Plasma nitriding can be influenced by process parameters such as temperature, time of treatment and gas mixture composition [5–8]. Several models have been proposed to explain the role of hydrogen in the nitriding process [9–13]. It was suggested that the N_2^+, N^+ and NH_x^+ ions were the active species in the nitriding process [9–11]. Haudis proposed that NH_x^+ ions are the species active in nitriding [9]. However, an experimental evidence shows that the active nitriding species are not ionic [10-13], and it is now well-known that nitriding can occur without the presence of hydrogen. The role of hydrogen was generally attributed to the enhancement of the nitrogen atom diffusion by removal of the surface oxides by a chemical mechanism, resulting in a thicker nitride-layer [14]. But a high concentration of hydrogen slows the nitriding process, resulting in a thinner nitrided layer [15]. In addition, it was shown in previous studies of N_2-H_2 discharges that with addition of H_2 in pure N_2 discharges, the secondary ionization coefficient increases [16-19]. This increase of secondary ionization coefficient caused higher concentration of active nitriding species than the pure nitrogen discharge [15]. The best results were achieved by N_2–H_2 (20-25 %) gas mixture. Increasing

the ratio of hydrogen to nitrogen further results in reduction of nitriding efficiency [15]. In this work, we report a study of cold radiofrequency plasma nitriding of unheated substrates of carbon steel C38 using two different gas mixtures (75% N_2/25% H_2 and 25% N_2/75% H_2). In our previous papers [20, 21], we have shown that such a treatment is very efficient for improving the corrosion resistance of C38 carbon steel in acidic medium. This enhancement is caused by the formation of nitrided phases on the steel surface after plasma treatment, which improves the corrosion resistance of C38 steel in 1 M HCl solution. In the case of N_2/H_2 mixture, a large enhancement of the corrosion resistance for the samples nitrided using only ~25 vol. % of hydrogen was obtained. Indeed, the inhibition efficiency reaches a maximum value of 98.5% for samples nitrided using 25 vol.% H_2 for 8 h of plasma nitriding. The aim of the present paper is to study the effect of the hydrogen addition on the mechanical properties of RF plasma-nitrided C38 carbon steel using Vickers microhardness test (Hv). Electron probe microanalysis (EPMA) and X-ray photoelectron spectroscopy (XPS) have been applied to characterize the nitride layer formed after plasma treatment.

2 Experimental details

2.1 Materials

The samples used in this study is a C38 carbon steel with chemical compositions (in mass %) of 0.370% C, 0.230% Si, 0.680% Mn, 0.016% S, 0.077% Cr, 0.011 % Ti, 0.059 %Ni, 0.009 % Co, 0.160 % Cu with the remainder being iron (Fe). Before nitriding, the carbon steel samples were mechanically polished by different grades of silicon carbide emery (120, 600 and 1200), and then manually polished with diamond paste (6 µm and 0.25µm) to

produce a fine surface finishing; degreased in acetone in an ultrasonic bath immersion for 5 min and then dried at room temperature before use.

2.2 Plasma nitriding

Non-heated C38 steel samples were plasma nitrided using cold radiofrequency plasma (13.56 MHz) generated by a EUROPLASMA CD 1200 set-up for different processing times on non-heated substrate. A schematic representation of the experimental set-up is given in our previous work [20]. A N_2/H_2 glow discharge was generated in an aluminium reactor chamber with a continuous power ranging from 0 to 600 W. The chamber was pumped down to 10.7 Pa using a pump Edwards (80 m^3/h), and the N_2/H_2 gas was introduced into the chamber. When the pressure became constant, the generator was switched on and adjusted to a certain power value, which gave rise to a continuous glow discharge. The plasma was created using a total constant flow of 500 sccm of N_2/H_2 gas mixtures 75% N_2/25% H_2 and 25% N_2/75% H_2 (vol.%) at a fixed power of 500 W.

2.3 Structural characterizations

The microstructural analysis was carried out using a Cameca SX100 Electron Probe Microanalysis (EPMA). Back-scattered electrons (BSE) images were taken with 15 kV, 10 nA. Nitrogen (N) X-ray profiles and quantifications were carried out at 10 kV, 400 nA. For profiles and quantifications, a PC2 crystal was used to detect the N Kα X-ray. Prior to analyse, the C38 steel substrates were carbon coated with a Bal-Tec SCD005 sputter coater.

The chemical composition of the nitrided layer and the chemical state of the various elements were investigated by X-ray photoelectron spectroscopy (XPS) on a VG ESCALAB 220 XL spectrometer. The monochromatized Al-Kα X-ray source ($h\nu$ = 1486.6 eV) was

operated in the CAE (constant analyser energy) mode (CAE = 150 eV for survey spectra and CAE = 30 eV for high resolution spectra), using the electromagnetic lens mode. The binding energy scale was initially calibrated using the Cu $2p_{3/2}$ (932.7 eV), Ag $3d_{5/2}$ (368.2 eV) and Au $4f_{7/2}$ (84 eV) peak positions, and internal calibration was referenced to the C 1s energy at 285 eV for aliphatic like species. Quantification of outer layers atomic composition and spectral simulation of the experimental peaks were achieved using the software provided by VG Scientific. XPS spectra were deconvoluted using a non-linear least squares algorithm with a Shirley base line and a Gaussian–Lorentzian combination. XPS Peak-Fit 4.1 software was used for all data processing.

2.4 Mechanical properties

Microhardness experiments were performed on the polished untreated and nitrided surfaces, using a microhardness tester equipped with a Vickers indenter using load of 5-100 g and a dwell time of 15 s. Five experiments were carried out in each case of sample and the mean value of Vickers microhardness is calculated for every substrate confirming the consistency in the results.

3 Results and discussion

3.1 Structural characterizations

Figure 1 shows back-scattered electron (BSE) image of N_2/H_2 (75% N_2/25% H_2) nitrided C38 steel in the case of 8h of plasma-treatment. The micrograph in the case of untreated C38 steel is also presented in order to facilitate comparison (fig. 1a) [22]. A black

layer can be seen on the edge of the nitrided steel substrates (Fig. 1b); as in BSE mode a darker colour indicates a lower atomic mass of atoms, this layer can be attributed to the presence of nitrogen. The micrographs show the formation of a uniform nitride layer after plasma nitriding N_2/H_2. For the sample nitrided in pure N_2 plasma, the thickness of the compound layer is about 10 µm [22]. When ~ 25 volumetric percent of hydrogen is added, the thickness of the compound layer increases and is about 15µm. However, scanning electron microscopy image for the sample treated in 25% N_2/75% H_2 (not shown) did not exhibit any significant nitrided layer, due to the lesser percentage of nitrogen in the gas mixture. This clearly demonstrates that the nitrided layer thickness depend on the hydrogen content in the plasma discharge. These results are coherent to those of the literature [15,23-24].

In order to complete this characterization, a quantitative profile of nitrogen was carried out from the inside of the sample towards the edge for N_2/H_2 plasma 8h nitrided C38 steel samples using the electron probe microanalysis (EPMA) (Figure 2). For all the analysed samples the highest concentration of nitrogen is that of the edge. Nitrogen profiles show that from the edge to the inside, nitrogen content decreases. This decrease is faster for 25% N_2/75% H_2 nitrided C38 steel sample in comparison to pure N_2 and 75% N_2/25% H_2 nitrided C38 steel samples under identical treatment conditions. The nitrogen concentration in the absence of hydrogen (pure N_2) is 2.02 %, with a nitrided layer of about 10 µm [22]. When ~25 vol. % of hydrogen is used, the nitrogen content is about 2.72 %, with a nitrided layer of about 15 µm. However, an excessive content of hydrogen (~75 vol. %) is not favourable to the formation of the nitride phases with a nitrogen concentration of about 0.44% and a nitrided layer of about 7 µm. Thus, the nitrogen content and the nitrided layer thickness mainly depend on the hydrogen content in the plasma discharge. Indeed, the use of hydrogen in a ~25 vol. % presents a combined role, first it increases the thickness of surface nitride layer (combined layer) by reducing the oxide layer [14, 24-26] and secondly during the

plasma treatment hydrogen increases the density of active nitriding species [15]. However, the increase of hydrogen content (~75 vol. %) induce a reduction of nitriding efficiency, which decreases the nitrogen content in the combined layer in comparison to the other studied plasma treatments. These results are in agreement with the literature [15,24].

XPS analysis was used to identify the elemental composition of the surface of N_2/H_2 plasma-nitrided C38. XPS spectra for untreated, pure N_2 and N_2/H_2 plasma 8h nitrided C38 steel substrates are previously described [20, 22]. The obtained values of binding energy (BE) are summarised in Tables 1. The values in parenthesis represent the relative percentage of the peak component.

From O 1s line deconvolution, oxygen appears in three chemical states (Table 1). The first peak located at lower binding energy (530.7 ± 0.2 eV) can be attributed to O^{2-}, and in principle could be related to the bond with Fe^{3+} in the Fe_2O_3 and/or Fe_3O_4 oxides [27]. The second peak located at approx. 531.7 ± 0.2 is ascribed to OH^-, and is attributable to oxygen in hydrous iron oxides, such as FeOOH and/ or $Fe(OH)_3$ [27]. Finally, the small peak may be assigned to the oxygen atom of adsorbed water with characteristic binding energy of 533.1 ± 0.2 eV [28].

The Fe 2p spectra for N_2/H_2 plasma-nitrided C38 steel surface were fitted using two doublets, 711 eV (Fe 2p3/2) and 724.1 eV (Fe $2p_{1/2}$), with an associated ghost structure [29]. The deconvolution of the high resolution Fe $2p_{3/2}$ XPS spectra for the all nitrided substrates shows that these peaks may be assigned as being due to iron in environments associated with iron nitride, iron oxide and hydroxide. Indeed, the first peak located at 707.4 eV for 75% N_2/25% H_2, 707 for 25% N_2/75% H_2, and 706.7 eV for pure N_2, was assigned to metallic iron (Fe^0) [30] and iron nitrides (Fe_xN) which corresponds to the nitride layer [31]. Inspection of these results (Table 1) shows that the plasma nitriding causes energy shifts of + 0.6 eV for pure N_2 (0vol% H_2), +1.3 eV for for 75% N_2/25% H_2 and + 0.9 eV for 25%

N_2/75% H_2 in the metallic Fe 2p photoelectron component. The second peak at a BE ~ 710.9 ± 0.2 eV assigned to Fe^{3+} as mentioned in [32], was attributed to ferric compounds such as FeOOH (i.e., oxyhydroxyde), Fe_2O_3 (i.e., Fe^{3+} oxide) and/or Fe_3O_4 (i.e., Fe^{2+}/Fe^{3+} mixed oxide) [33,34], while that located at 715.0 ± 0.2 eV may be ascribed to the satellite of Fe(II) [22,35]. The last peak, observed at 720.3 ± 0.4 eV is ascribed to the satellites of the ferric compounds as mentioned previously [36].

The deconvoluted N 1s spectra for N_2/H_2 plasma-nitrided C38 steel substrates show three main peaks corresponding to three distinct species of nitrogen (Table 1). The first peak located at approx. 397.2 ± 0.1 eV has the largest contribution and is attributed to iron nitrides (Fe_xN) [37,38]. The second component is assigned to C−N bonding at 398.5 ± 0.3 eV [39]. The last peak at higher binding energy (400.4 ± 0.2 eV) is attributed to the N−O bonding (oxidized nitrogen) as a result of the oxidation of the nitrogen in the nitride layer [40]. The XPS nitrogen quantification confirms the EMPA nitrogen quantification. Indeed, the nitrogen concentration present on the N_2/H_2 plasma-nitrided C38 steel surface is about 5.00 wt.% for 75% N_2/25% H_2, 1.47 wt.% for 25% N_2/75% H_2, and 1.87 wt.% for pure N_2.

Therefore, based on the present XPS and EPMA results, we can conclude that an homogeneous and uniform nitride layer is formed using nitrogen-hydrogen radiofrequency plasma discharge without heating the C38 substrate.

3.2 Hardness of nitrided layer

In order to study the effect of hydrogen addition on the mechanical properties of nitrided plasma N_2/H_2 for 8 hours, microhardness measurements were made at a load of 5 g applied for 15 s. The results are shown in Fig. 3. Each point, given in this figure is the average of five measurements at different places on the sample. The uncertainties shown are derived

from the variation in the five values, and therefore include a component arising from the variation in hardness over the surface. We have previously reported the variation of microhardness with treatment time for the case of treatments in pure nitrogen [22]. We have demonstrated that the treatment in N_2 plasma is very efficient for improving the mechanical properties of C38 carbon steel. Indeed, the microhardness values increase as the plasma-processing time increases to reach 1487 $HV_{0.005}$ using plasma treatment time of 8 hours. This correlates with results presented in Fig. 3, in which the microhardness values increase after nitriding plasma N_2/H_2. The nitrided plasma sample 75%N_2/25%H_2 reaches a maximum value of more than 2242 $HV_{0.005}$, this value is higher compared to that of pure N_2 (1487 $HV_{0.005}$) and 75% N_2/25% H_2 (1057 $HV_{0.005}$) nitrided C38 steel samples under identical treatment conditions. S. Kumar et al. reported a maximum value for the surface hardness of sample nitrided using 25 vol. % of H_2 [24]. Similar results have been obtained previously [15]. The beneficial effect of the hydrogen addition (25 vol.%) to provide higher mechanical properties of C38 steel can be explained by the enhancement of the nitrogen atom diffusion as explained in structural section. The sample treated with an excessive amount of hydrogen (~75%) in the gas mixture does not present a gain in hardness compared to the one treated in pure nitrogen.

In order to complete this study, the microhardness profile at different loads of 5, 10, 15, 25, 50 and 100g were applied. Fig. 4 shows the microhardness values of the untreated and the plasma treated N_2/H_2 samples for 8h of plasma treatment as a function of the applied load. The profile for untreated and pure N_2 plasma-nitrided C38 steel substrates is also presented in order to facilitate comparison [22]. Figure 4 shows that the obtained hardness values depend on the applied load. It is seen that the microhardness values decrease with increasing the applied load for all treated samples. Such behaviour can be explained by the fact that the indentation depth increases with applied load leading to a higher contribution of unmodified

part of the substrate to the measured hardness. These results agrees well with literature [42-46]; and hardness decrease with the load is known as the "indentation size effect" (ISE) [47].

4 Conclusion

In this work C38 carbon steel samples were nitrided using N_2/H_2 gas mixtures in cold radiofrequency plasma. The treated layer shows better mechanical properties than the untreated. At higher amount of hydrogen (~75 vol. %) in the gas mixture, the rate of the nitriding process is slowed down, resulting in a reduced nitrided layer thickness and no gain in hardness compared with the treatment in pure N_2. The addition of hydrogen at a concentration of ~25 vol. % produces layers with higher nitrogen content. Moreover, a thicker nitrided layer is formed compared to pure N_2 and 25% N_2/75% H_2 nitrided C38 steel samples leading to the formation of a harder surface. Indeed, the surface hardness achieves, for a plasma processing time of 8 hours, a value of 2242 $HV_{0.005}$ for such treatment. Moreover a decrease in the hardness values with the applied load has been evidenced. Such behaviour is explained by a higher contribution of unmodified part of the substrate to the measured hardness.

References

1. L. Chekour, C. Nouveau, A. Chala, M.A. Djouadi,Wear. **255,** 1438 (2003)
2. P. Steyer, J.-P. Millet, S. Anderbouhr, P. Jacquot, Surf. Eng. **17**, 327 (2001)
3. K.H. Lee, K.S. Nam, P.W. Shin, D.Y. Lee, Y.S. Song, Mater. Lett. **57**, 2060 (2003)
4. A. Alsaran, H. Altun, M. Karakan, A. Celik, Surf. Coat. Technol. **176**, 344 (2004)
5. A. Alsaran, A. Celik, C. Celik, Surf. Coat. Technol. **160**, 219 (2002).
6. L. Marot, L. Pichon, M. Drouet, A. Straboni, Mater. Lett. **44**, 35 (2000).
7. A. Alsaran, Mater. Charact. **49**, 171 (2003)
8. M. Sahara, T. Sato, S. Ito, K. Akashi, Mater. Chem. Phys. **54**, 123 (1998)
9. M. Hudis, J. Appl. Phys. **44**, 1489 (1973)
10. G.G. Tibbetts, J. Appl. Phys. **46** 5072 (1974)
11. L. Petitjean, A. Ricard, J. Phys. D: Appl. Phys. **17,** 919 (1984)
12. A. Szasz, D.J. Fabian, A. Hendry, Z. Szazne-Csih, J. Appl. Phys. **66**, 5598 (1989)
13. A. Ricard, J.E. Oseguera-Pena, L. Falk, H. Michel, M. Gantois, IEEE Trans. Plasma Sci. **18**, 940 (1990)
14. C.A. Figueroa, D. Wisnivesky, F. Alvarez, J. Appl. Phys. **92**, 764 (2002)
15. J.M. Priest, M.J. Baldwin, M.P. Fewell, Surf. Coat. Technol. **145**, 152 (2001)
16. R. Nagpal, A. Garscadden, Chem. Phys. Lett. **231**, 211 (1994)
17. A. Garscadden, R. Nagpal, Plasma Sources Sci. Technol. **4**, 268 (1995)
18. B. Gordiets, C.M. Ferreira, M.J. Pinheiro, A. Ricard, Plasma Sources Sci. Technol. **7**, 363 (1998)
19. B. Gordiets, C.M. Ferreira, M.J. Pinheiro, A. Ricard, Plasma Sources Sci. Technol. **7,** 379 (1998)
20. F.Z. Bouanis, C. Jama, F. Bentiss, M. Traisnel, Corrosion Science. **52**, 3180 (2010)
21. F.Z. Bouanis, F. Bentiss, M. Traisnel, C. Jama, Electrochim. Acta. **54**, 2371 (2009)
22. F.Z. Bouanis, F. Bentiss, S.Bellayer, J.B. Vogt, C. Jama, Mat. Chem.Phys. 127, 329 (2011).
23. A. Chala, L. Chekour, C. Nouveau, C. Saied, M.S. Aïda, M.A. Djouadi, Surf. Coat. Technol. **200**, 512 (2005)
24. S. Kumar, M.J. Baldwin, M.P. Fewell, S.C. Haydon, K.T. Short, G.A.Collins, J. Tendys, Surf. Coat. Technol. **123**, 29(2000)
25. F. Borgioli, A. Fossati, E. Galvanetto, T. Bacci, Surf. Coat. Technol. **200**, 2474 (2005)

26. M.P. Fewell, J.M. Priest, M.J. Bladwin, G.A. Collins, K.T. Short, Surf. Coat. Technol. **131**, 284 (2000)
27. W. Temesghen, P.M.A. Sherwood, Anal. Bional. Chem. **373**, 601 (2002)
28. K. Babić-Samardžija, C. Lupu, N. Hackerman, A.R. Barron, A. Luttge, Langmuir **21**, 12187 (2005)
29. M. Lebrini, M. Lagrenée, M. Traisnel, L. Gengembre, H. Vezin, F. Bentiss, Appl. Surf. Sci. **253**, 9267 (2007)
30. R. Devaux, D. Vouagner, A.M. De Becdelievre, C. Duret-Thual, Corros. Sci. **36,** 171 (1994).
31. L.C. Gontijo, R. Machado, E.J. Miola, L.C. Casteletti, P.A.A. Nascente, Surf. Coat. Technol. **183**, 10 (2004)
32. M. Lebrini, M. Lagrenée, M. Traisnel, L. Gengembre, H. Vezin, F. Bentiss, Appl. Surf. Sci. **253**, 9267 (2007)
33. O. Olivares, N.V. Likhanova, B. Gomez, J. Navarrete, M.E. Llanos-Serrano, E.Arce, J. M. Hallen, Appl. Surf. Sci. **252**, 2894 (2006)
34. M.A. Pech-Canul, P. Bartolo-Perez, Surf. Coat. Technol. **184**, 133 (2004)
35. R.K. Tandon, R. Payling, B.E. Chenhall, P.T. Crisp, J. Ellis, R.S. Baker, Appl. Surf. Sci. **20**, 527 (1985).
36. S. Ciampi, V. Di Castro, Surf. Sci. **331**, 294 (1995)
37. S.P. Hong, K.H. Kim, Surf. Coat. Technol. **122**, 260 (1999)
38. X. Wang, W.T. Zheng, H.W. Tian, S.S. Yu, W. Xu, S.H. Meng, X.D He, J.C. Han, C.Q. Sun, B.K. Tay, Appl. Surf. Sci. **220**, 30 (2003)
39. C. Jama, O. Dessaux, P. Goudmand, J.-M. Soro, D. Rats, J. Von Stebut, Surf. Coat. Technol. **116**, 59 (1999)
40. F. Kieckow, C. Kwietniewski, E.K. Tentardini, A. Reguly, I.J.R. Baumvol, Surf. Coat. Technol. **201**, 3066 (2006)
41. U. Figeroa, J. Oseguerra, P.S. Schabes-Retchkiman, Surf. Coat.Technol. **86–87,** 728 (1996)
42. M. Raaif, F.M. El-Hossary, N.Z. Negm, S.M. Khalil, P. Schaaf, J. Phys.: Cond. Mat. **19**, 396003 (2007)
43. M.S. Shah, M. Saleem, R. Ahmad, M. Zakaullah, A. Qayyum, G. Murtaza, J. Mat. Process. Technol. **199**, 363 (2008)
44. S. Rudenia, J. Pan, I.O. Wallinder, C. Leygraf, P. Kulu, V. Milkli, J. Vac. Sci. Technol. A**19,** 1425 (2001)

45. K. Kawata, H. Sugimura, O. Takai, Thin Solid Films **390**, 64 (2001)
46. R. Lòpez-Callejas, A.E. Muňoz-Castro, R. Valencia A, S.R. Barocio, E.E. Granda-Gutiérrez, O.G. Godoy-Cabrera, A. Mercado-Cabrera, R. Peňa-Eguiluz, A. Piedad-Beneitez, Vacuum **81**, 1385 (2007)
47. A. Iost, J.B. Vogt, Scripta Materialia **37**, 1499 (1997)

Figure captions

Fig. 1. Cross section images of untreated and 8h nitrided steel samples. a) Back Scattering electron photograph (BSE) of untreated steel, and b) BSE micrograph of 75% N_2/25% H_2 nitrided C38 steel.

Fig. 2. Nitrogen quantification along a line from the inside of the N_2/H_2 nitrided C38 steel substrates to the edge: □) 75% N_2/25% H_2, Δ) pure N_2 and ○) 25% N_2/75% H_2.

Fig. 3. Variation of microhardness of C38 steel samples nitrided for 8h with the percentage hydrogen in the N_2/H_2 gas mixture**.** The values in the bracket present the "d" arithmetic mean of the two diagonals, d_1 and d_2.

Fig. 4. Variation of the microhardness of the untreated and N_2/H_2 plasma 8h nitrided C38 steel substrates (0%, 25% and 75% of hydrogen) as function of the applied loads.

Table 4.

Binding energies (eV), relative intensity and their assignment for the major core lines observed for N_2/H_2 plasma 8h nitrided C38 steel substrates.

Substrate	N 1s		O 1s		Fe 2p	
	BE (eV)	Assignment	BE (eV)	Assignment	BE (eV)	Assignment
75% N_2/25% H_2 [20]	397.3 (43 %)	Fe_xN	531.2 (47 %)	Fe_2O_3/ Fe_3O_4	707.4 (45%)	Fe^0, Fe_xN
	398.7 (30 %)	CN	5317 (44 %)	$FeOOH/Fe(OH)_3$	711.0 (17 %)	Fe_2O_3/FeOOH/ $Fe(OH_3)$
	400.3 (27 %)	NO	532.9 (9 %)	Adsorbed H_2O	715.3 (8 %)	Satellite of Fe(II)
					720.7 (21 %)	Satellite of Fe(III)
					724.5 (9 %)	Fe $2p_{1/2}$
25% N_2/75% H_2 [20]	397.2 (51 %)	Fe_xN	530.9 (31 %)	Fe_2O_3	707 (46 %)	Fe^0, Fe_xN
	398.3 (40 %)	CN	531.7 (44 %)	$FeOOH/Fe(OH)_3$	711.1 (18 %)	Fe_2O_3/FeOOH/ $Fe(OH_3)$
	400.4 (9 %)	NO	532.5 (25 %)	Adsorbed H_2O	714.8 (6 %)	Satellite of Fe(II)
					720.5 (21 %)	Satellite of Fe(III)
					725 (9 %)	Fe $2p_{1/2}$
pure N_2 [21]	397.3 (45 %)	Fe_xN	530.3 (34 %)	Fe_2O_3	706.7 (44 %)	Fe^0, Fe_xN
	398.8 (38 %)	CN	531.5 (42 %)	$FeOOH/Fe(OH)_3$	710.8 (13 %)	Fe_2O_3/FeOOH/ $Fe(OH)_3$
	400.7 (17 %)	NO	533.0 (24 %)	Adsorbed H_2O	715.1 (12 %)	Satellite of Fe(II)
					719.9 (23 %)	Satellite of Fe(III)
					724.2 (8 %)	Fe $2p_{1/2}$

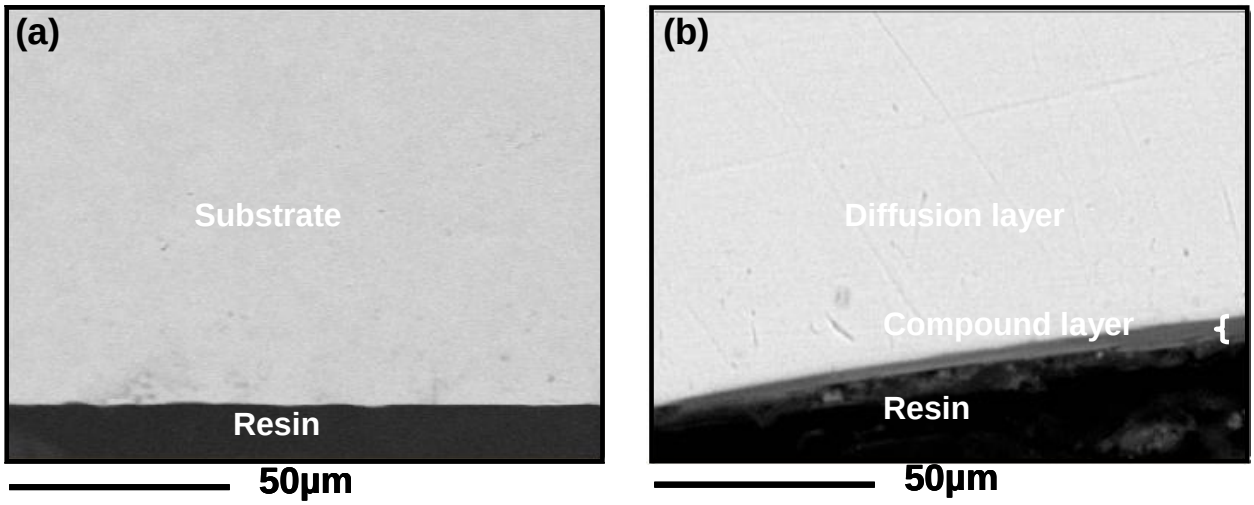
(a)
Substrate
Resin
50μm
(b)
Diffusion layer
Compound layer
Resin
50μm

Figure 1

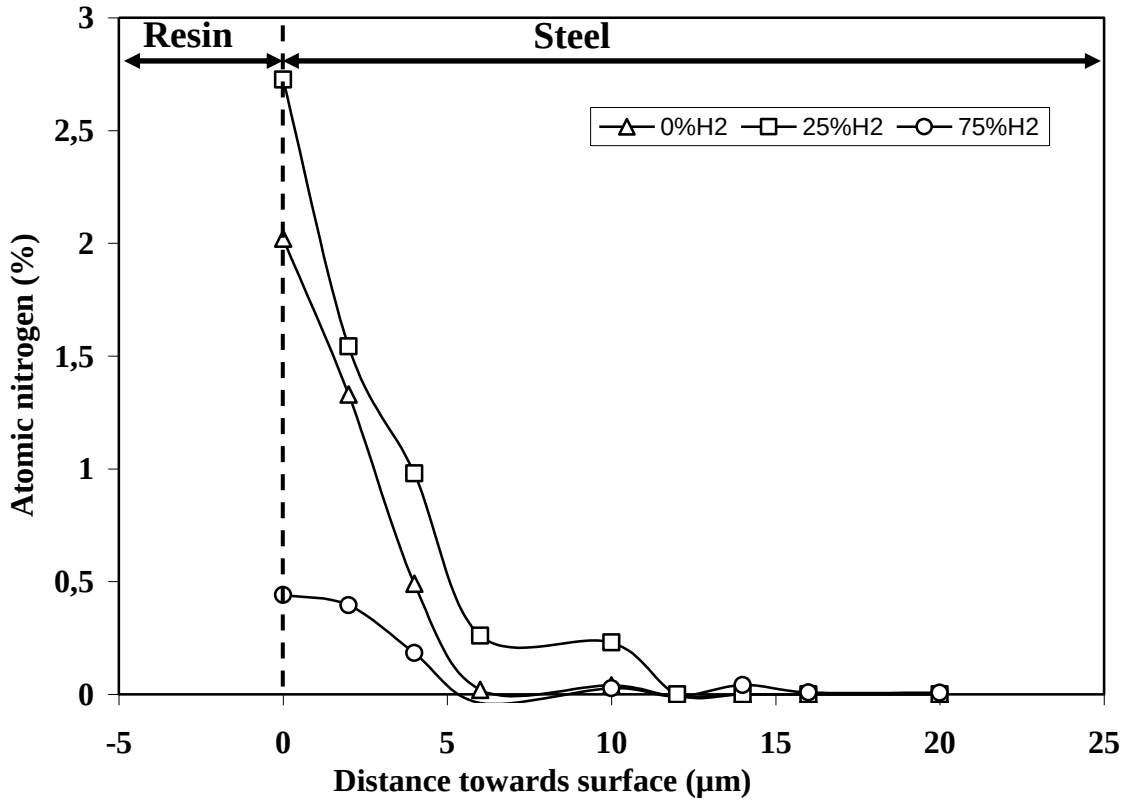
Resin
Steel
0%H2
25%H2
75%H2
Atomic nitrogen (%)
3
2,5
2
1,5
1
0,5
0
-5
0
5
10
15
20
25
Distance towards surface (µm)

Figure 2

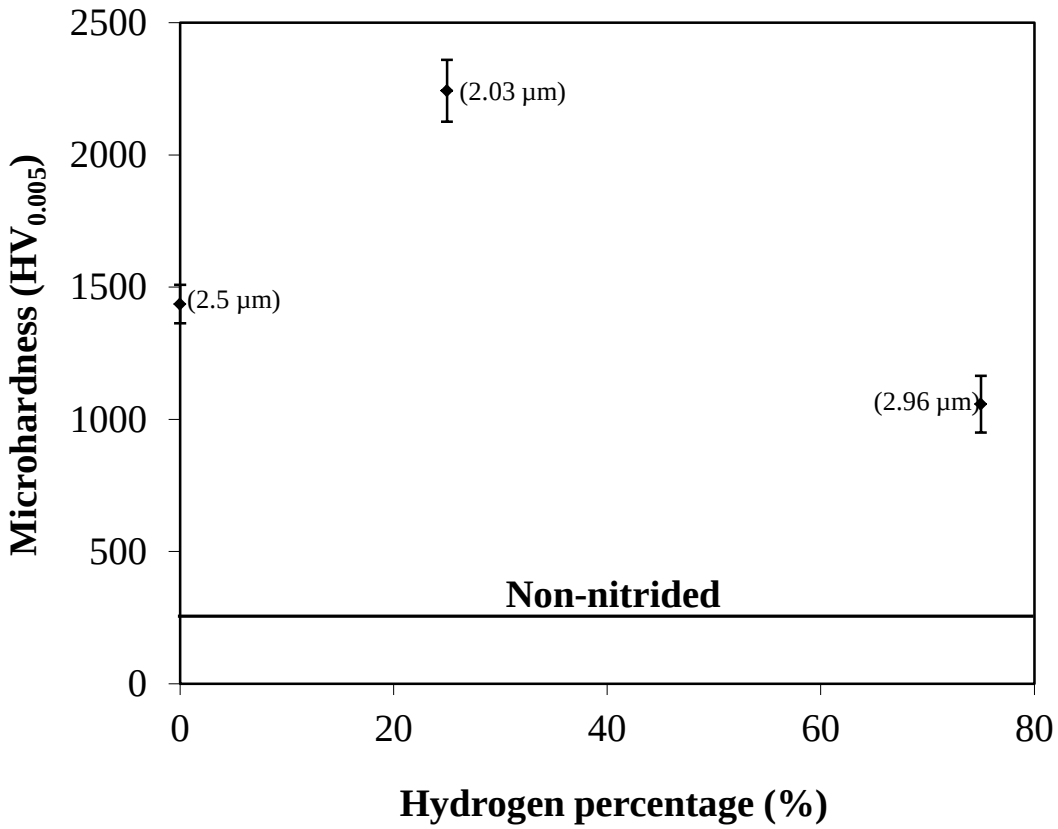
2500
2000
1500
1000
500
0
Microhardness (HV0.005)
(2.03 µm)
(2.5 µm)
(2.96 µm)
Non-nitrided
0
20
40
60
80
Hydrogen percentage (%)

Figure 3

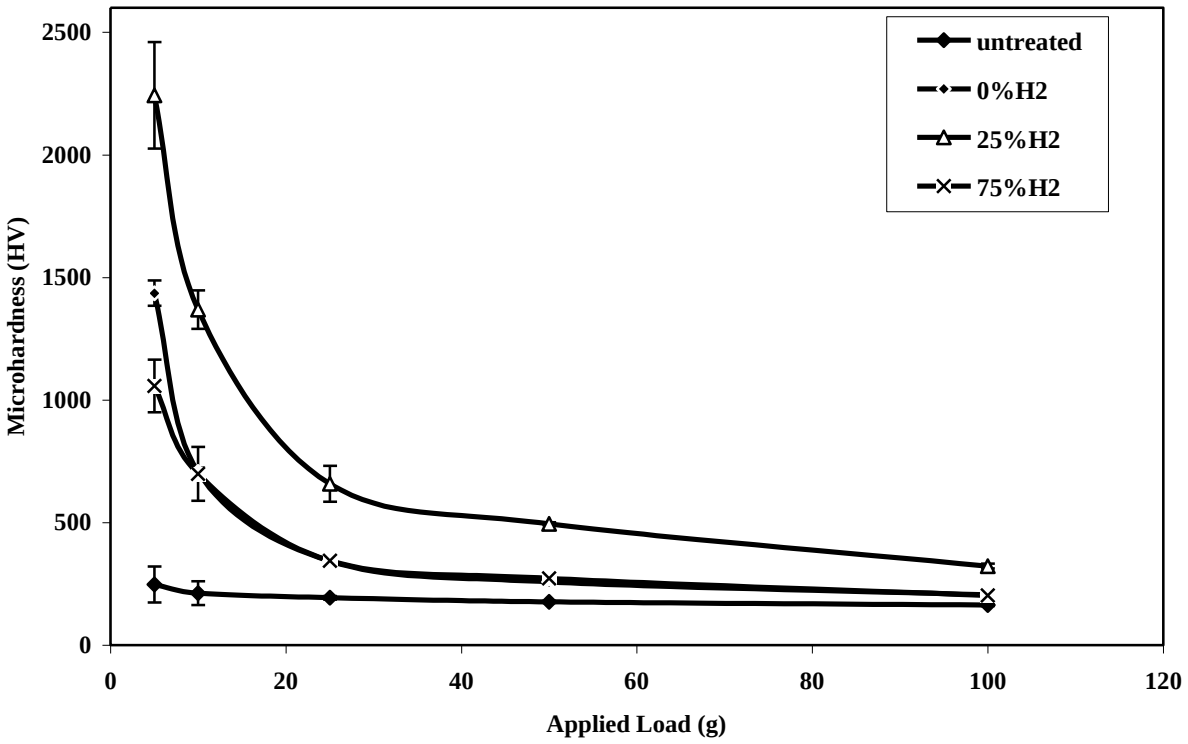
2500
2000
1500
1000
500
0
Microhardness (HV)
0
20
40
60
80
100
120
Applied Load (g)
untreated
0%H2
25%H2
75%H2

Figure 4